

Supplemental Methods

Fifteen 6-7 weeks old nude mice were anesthetized using isoflurane inhalation and injected with ^{18}F -C-SNAT (6.45 ± 0.58 MBq, $n=15$) as described in the Positron Emission Tomography protocol in the main text of the manuscript. They were kept under anesthesia until euthanized by cervical dislocation at different times (1-170 min) after tracer administration. Blood was collected from the neck into a heparinized test tube, and the plasma was separated by centrifugation. Plasma (50 μL) was counted in a Packard Cobra II gamma counter together with a diluted sample of ^{18}F -C-SNAT. Ten of the fifteen samples were further processed for radioactive metabolite analysis by HPLC (Supplemental Fig. 3b).

The total and metabolite corrected concentration of ^{18}F -C-SNAT in plasma was compared to the image-derived input function generated from the left ventricular region of the combined PET/CT images. All three curves were fitted to an exponential decay function ($Y = (Y_0 - \text{Plateau}) \cdot e^{-kx}$) from their initial peak activity.

Supplemental Results

The image-derived input function from tumor-bearing nude mice was comparable with the *ex vivo* input function obtained from healthy nude mice (Supplemental Fig. 3a). There is no evidence of tracer retention in the left heart ventricle of any mice. RadioHPLC analysis of plasma taken from healthy nude mice revealed 95.1% parent compound at 10 min, 15.2% parent compound at 63 min, and 1.2 % parent compound at 119 min (Supplemental Fig. 3b). In addition, the major radiolabeled metabolite (reduced ^{18}F -C-SNAT) is present at 69.9% at 63 min and 63.3% at 119 min. We have previously shown that ^{18}F -C-SNAT is metabolized in mouse serum while *cyclic*- ^{18}F -C-SNAT remained stable (1).

Supplemental Discussion

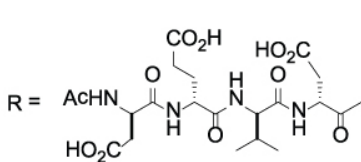
Using an image-derived input function is essential in quantitative mouse microPET imaging, since it is not feasible to make an individual arterial input function due to limited blood volume — a typical nu/nu mouse of 20 gram holds around 2 mL of blood. Multiple samplings would critically reduce the blood volume. Image-derived input function in mice must model the concentration of injected activity over time and has been used successfully with other tracers like ^{18}F -FDG (2–4) and ^{18}F -FLT (5). Alternatively, a reference region approach (6) using the muscle or similar tissue to determine the delivery of tracer could be taken, however it should be confirmed that the reference region is truly free from tracer retention. This point should be kept in mind when interpreting the common measurement of tumor/muscle ratio. In this study, ^{18}F -C-SNAT did not show signs of specific retention in the ventricle, which is similar to the *ex vivo* input function. This region can therefore be used as an estimated image-derived input function.

^{18}F -C-SNAT is relatively stable in mice (95.1% parent compound at 10 min) and the associated metabolites (Supplemental Fig. 3b) are all less lipophilic than the parent compound and *cyclic*- ^{18}F -C-SNAT. The major metabolite is reduced ^{18}F -C-SNAT which would function similarly as ^{18}F -C-SNAT and together these two compounds account for a total of 64.5% (63.3% reduced ^{18}F -C-SNAT + 1.2% ^{18}F -C-SNAT) at 119 minutes of the active radiolabelled compounds.

Supplemental References

1. Shen B, Jeon J, Palner M, et al. Positron emission tomography imaging of drug-induced tumor apoptosis with a caspase-triggered nanoaggregation probe. *Angew Chem Int Ed Engl.* 2013;52:10511-10514.
2. Kim J, Herrero P, Sharp T, et al. Minimally invasive method of determining blood input function from PET images in rodents. *J Nucl Med.* 2006;47:330-336.
3. Kudomi N, Bucci M, Oikonen V, et al. Extraction of input function from rat [^{18}F]FDG PET images. *Mol Imaging Biol.* 2011;13:1241-1249.

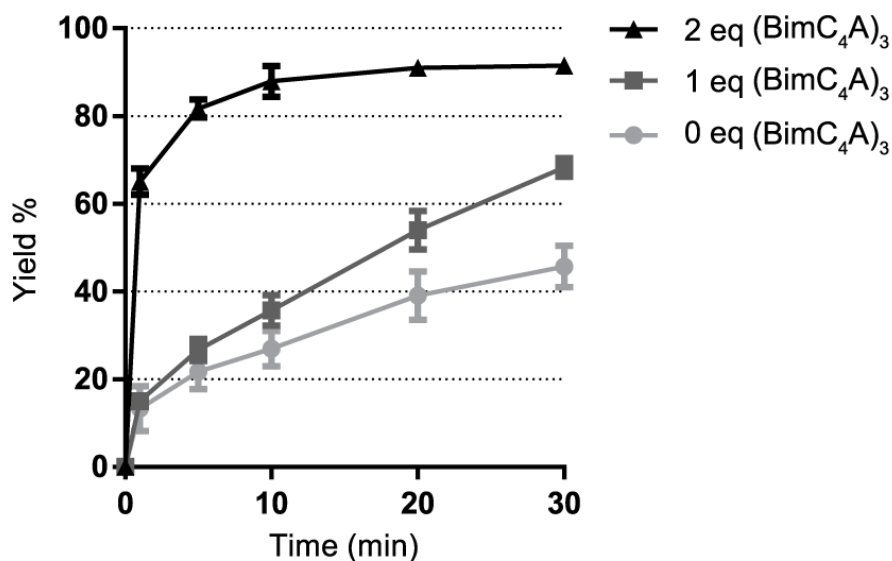
4. Tantawy MN, Peterson TE. Simplified [18F]FDG Image-Derived Input Function Using the Left Ventricle , Liver , and One Venous Blood Sample. *Mol Imaging*. 2010;9:76-86.
5. Kim SJ, Lee JS, Im KC, et al. Kinetic modeling of 3'-deoxy-3'-18F-fluorothymidine for quantitative cell proliferation imaging in subcutaneous tumor models in mice. *J Nucl Med*. 2008;49:2057-2066.
6. Zanderigo F, Ogden RT, Parsey R V. Reference region approaches in PET : a comparative study on multiple radioligands. *J Cereb Blood Flow & Metab*. 2013;33:888-897.



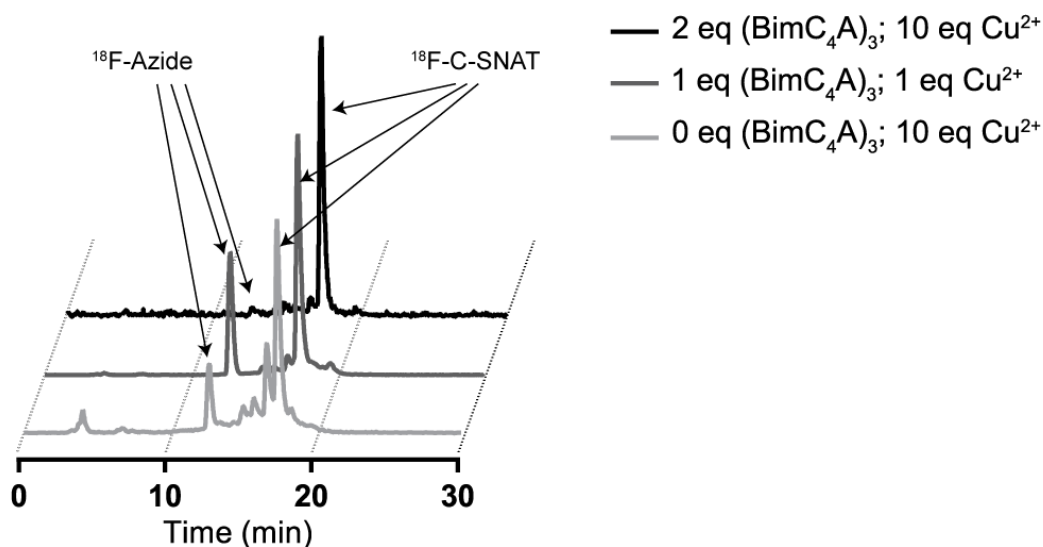
$(\text{BimC}_4\text{A})_3 =$

Chemical structure of the BimC₄A monomer, showing a benzimidazole core with a 4-carboxybutyl chain (COOK) and a trimethylammonium group (N⁺).

A CuAAC reaction kinetics

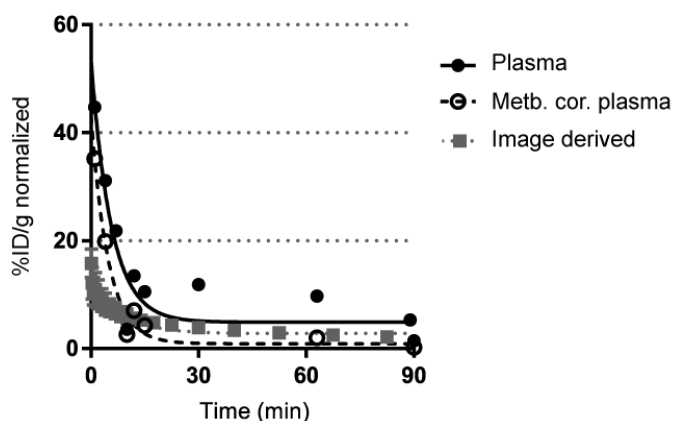


B Radio-HPLC of three reaction conditions

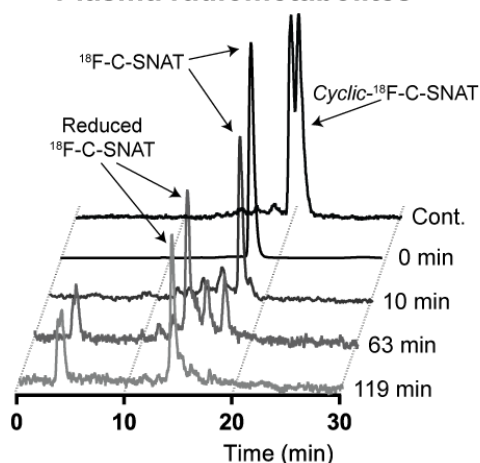


Supplemental Figure 2 – A) Comparison of CuAAC reaction kinetics for ¹⁸F-labeling after different reaction times; B) Comparison of radio-HPLC traces under three reaction conditions: 2 eq. (BimC₄A)₃ and 10 eq. Cu²⁺ after 10 minutes of reaction; 1 eq. (BimC₄A)₃ and 1 eq. Cu²⁺ after 30 minutes of reaction; and 10 eq. Cu²⁺ without (BimC₄A)₃ after 30 minutes of reaction.

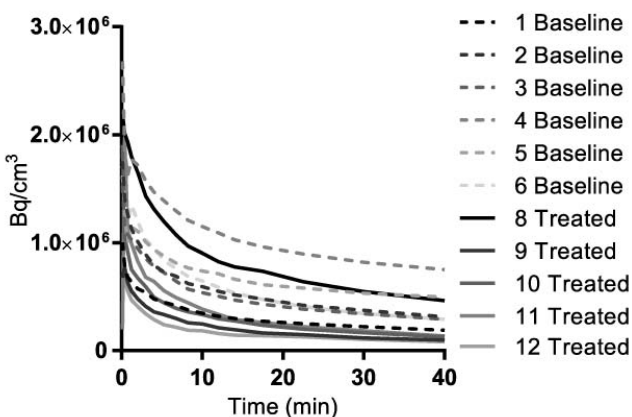
A Comparison of input functions



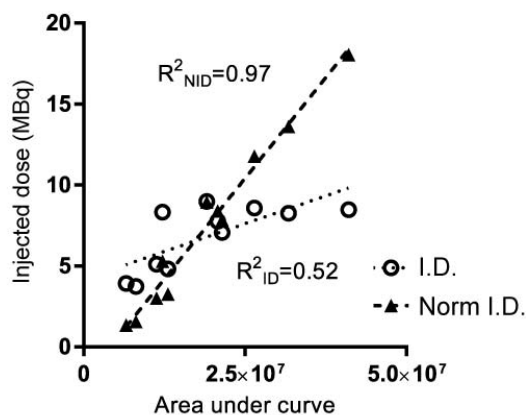
B Plasma radiometabolites



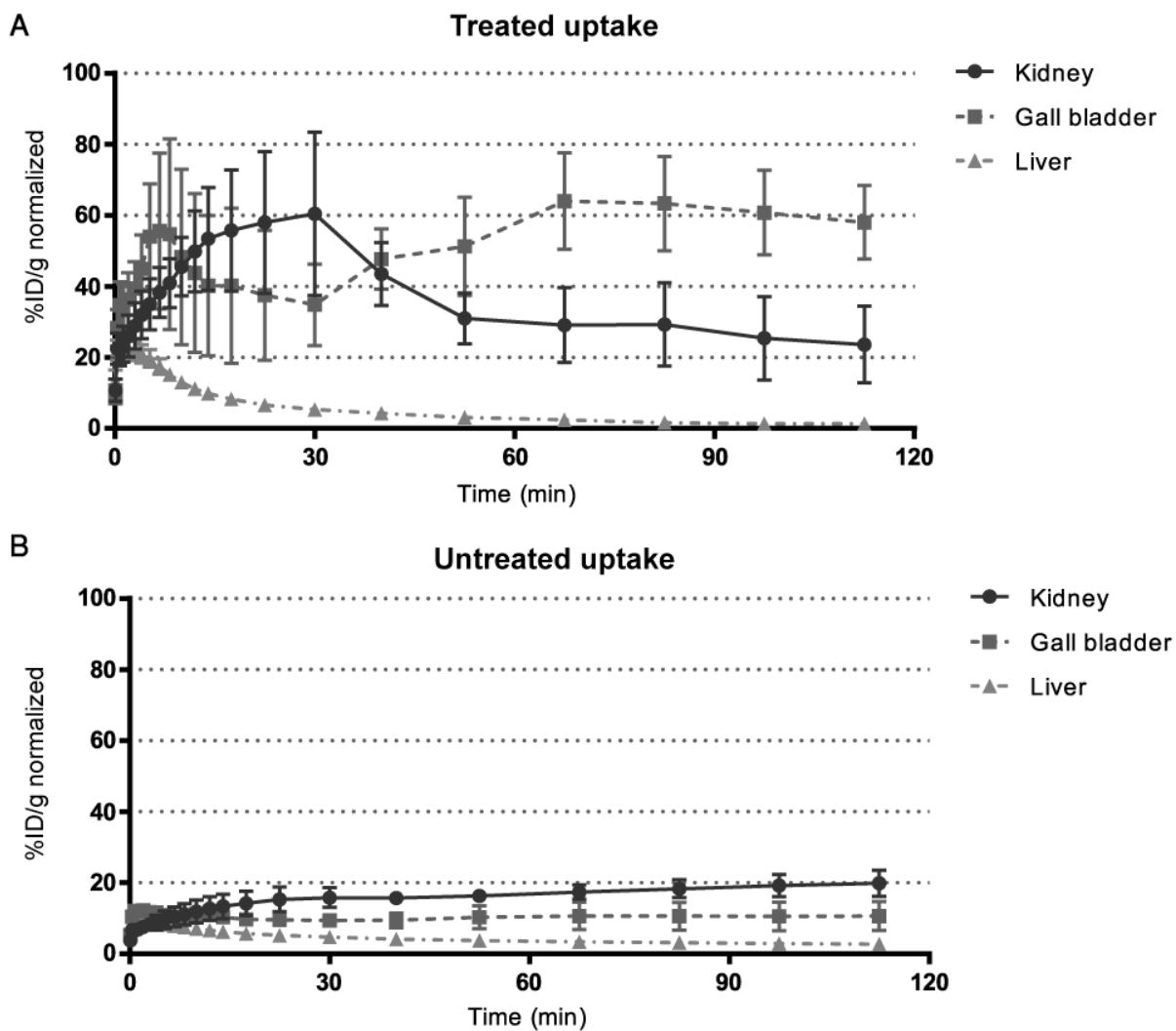
C Heart time-activity curves



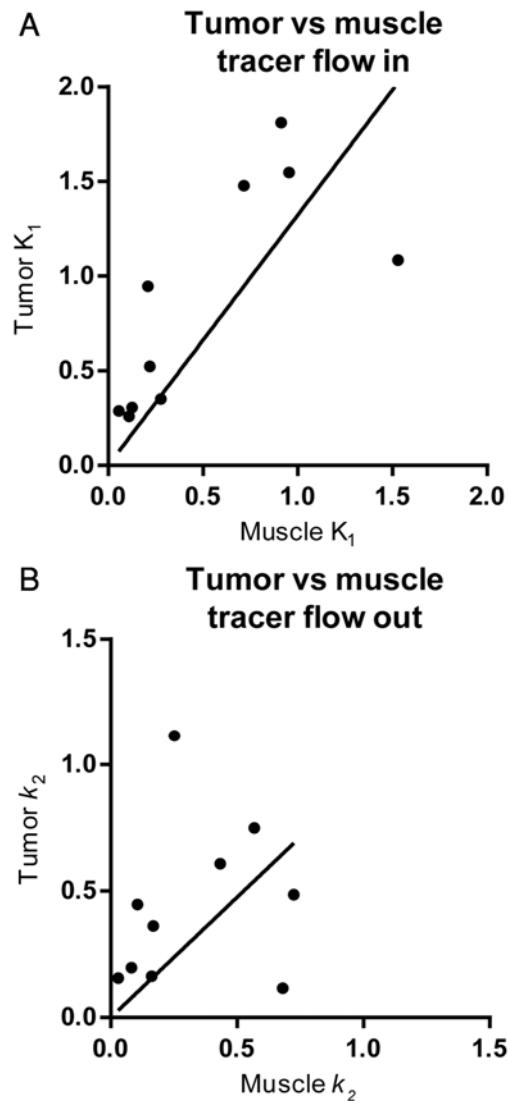
D Normalisation of injected dose



Supplemental Figure 3 – Input functions, metabolites and normalization of injected dose. A) Comparison between *ex vivo* plasma input function, metabolite corrected *ex vivo* plasma input function and image-derived input function. B) Radio-HPLC trace of plasma radioactivity, sampled at 10 min, 63 min and 119 min, compared to standards of *cyclic*-¹⁸F-C-SNAT (Cont.) and ¹⁸F-C-SNAT (0 min); the major metabolite is reduced tracer. C) Activity in the left heart ventricle of each mouse over the first 40 minutes. D) Injected dose vs. area under the left heart ventricular input function, before and after normalization.



Supplemental Figure 4 – Time activity curves of ^{18}F -C-SNAT in liver, kidney and gallbladder of treated (A) and untreated (B) mice.



Supplemental Figure 5 – Comparison between blood flow changes in tumor and muscle following chemotherapeutic treatments. A) K_1 in tumor vs K_1 in muscle; there is a correlation between changes in blood flow in both tissues. B) k_2 in tumor vs k_2 in muscle; there is no correlation between the two tissues, as expected, since there is accumulation in the tumor tissue and no accumulation in the muscle.